Heat and Mass Transfer (2019) 55:2651–2666
https://doi.org/10.1007/s00231-019-02605-1

ORIGINAL

Experimental investigations on thermal performance of solar air heater with wavy fin absorbers

Abhishek Priyam [1] · Prabha Chand [2]

Received: 27 November 2017 / Accepted: 5 March 2019 / Published online: 18 March 2019

Abstract

In this paper, the thermal performance of wavy finned solar air heater are investigated experimentally. Experiments were performed under Jamshedpur (22° 48' N, 86° 11′ E) prevailing weather conditions. The effect of mass flow rate, fin spacing and insolation on thermal efficiency and air temperature rise of wavy fin solar air heaters are investigated. The results showed that the maximum efficiency of 69.55% has been found for the mass flow rate 0.0158 kg/s and fin spacing of 2 cm. Further, for the same fin spacing, maximum air temperature rise has been obtained as 64.33°C at the mass flow rate of 0.00312 kg/s. For the range of mass flow rate (0.00312–0.0158 kg/s) and fin spacing (2–6 cm), the wavy fin absorber solar air heater has been found to be 67.44 to 121.43% thermally efficient. These experimental results would be reliable and useful for optimum design in practical applications.

Nomenclature

$\overline{h}$	Heat transfer coefficient (W/m^2 -K)
A_c	Collector area (m^2)
F′	Collector efficiency factor
F_R	Collector heat removal factor
I	Insolation (W/m^2)
T_i	Inlet air temperature (K)
T_{pm}	Mean temperature of absorber plate(K)
η	Thermal efficiency
$(\tau\alpha)$	Transmittance absorptance product
ΔT	Rise in temperature (K)
T_o	Outlet air temperature (K)
$\dot{m}$	Mass flow rate of air (kg/s)
A	Total heat transfer area (m^2)
C_p	Specific heat of air (J/kg-K)
T_{fm}	Mean temperature of air (K)
C_d	Coefficient of discharge
$\overline{h}A$	Thermal conductance (W/K)
U_L	Total loss coefficient (W/m^2 -K)

1 Introduction

Solar energy is considered as an optimistic and green source of energy and also used for many industrial and domestic applications. In solar energy exertions, solar air heaters provide the moderate air temperatures and used for the drying of crops, space heating etc. [1]. The performance of plane solar air heater is found to be low due to the lower heat transfer coefficient between the absorber plate and the air flowing through the duct and thus leads to higher thermal losses to the ambient [2]. In order to improve the heat transfer rate in the solar air heater, fins, fins with baffles, artificial roughness and packed beds are introduced in the flow channel. Thermal performance of heat pipe flat plate solar collector with cross flow heat exchanger was investigated by Lan et al. [3]. They proposed a theoretical model and validated with the experimental and numerical results. They also analyzed and discuss the influence of relevant parameters on the thermal performance of heat pipe flat plate solar collector. Fins are the extended surfaces attached to the absorber plate to increase the heat transfer area, thus increases the heat transfer rate. Numerous research on heat transfer characteristics of fins, such as plain, wavy, offset and louvered fins over the flat plate has been studied and a considerable augmentation in heat transfer took place. Hence, researchers have focused their attention to employ these fins in the air heater. Wavy fins are uninterrupted fin surfaces with cross-sectional shapes similar to rectangular fins, but with cyclic lateral shifts, perpendicular to the flow direction. The resulting waveform provides effective

✉ Abhishek Priyam
priyamanik06@gmail.com

[1] Department of Mechanical Engineering, MPSTME, NMIMS University, Mumbai 400056, India

[2] Department of Mechanical Engineering, N.I.T Jamshedpur, Jamshedpur, Jharkhand 831014, India

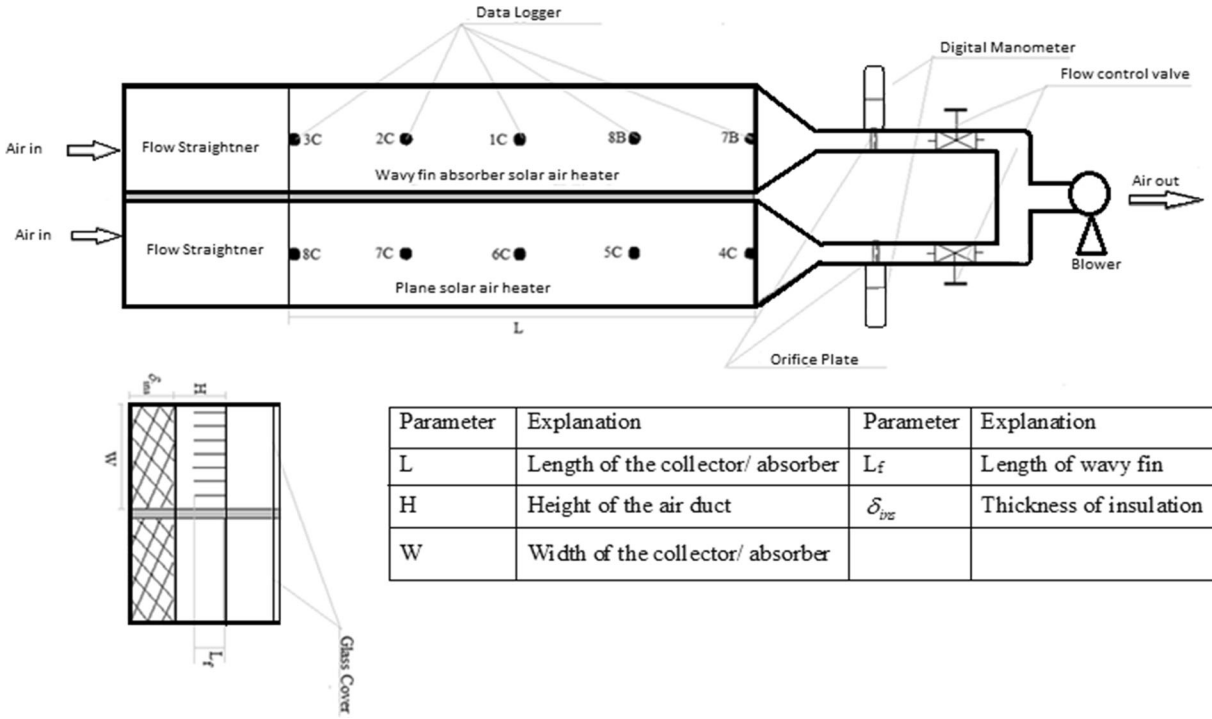

Parameter	Explanation	Parameter	Explanation
L	Length of the collector/ absorber	L_f	Length of wavy fin
H	Height of the air duct	δ_{ins}	Thickness of insulation
W	Width of the collector/ absorber		

Fig. 1 Schematic Diagram of Experimental set up

interruptions and induces a complex flow field. These counter rotating vortices form while the fluid passes over the concave wave surfaces and produce a corkscrew like flow pattern [4].

So, the wavy fin is a promising element to provide superior performance with considerable pressure drop. Heat transfer and pressure drop characteristics of wavy fin and flat tube heat exchangers have been analyzed to develop the correlations by junqi et al. [5]. Synder et al. [6] investigated on a wavy channel with circular arcs similar to the geometry presented by Kays and London [7] to minimize flow separation. They found an increase in heat transfer rate by a factor 9 and 14 in air and water respectively. Garg and Maji [8] used finite- difference solution for laminar viscous flow in a wavy channel. Backflow and flow reversal were found with the variation of wall pitch ratio. An extensive work by Nishimura et al. [9] showed the formation of recirculation vortex in the laminar flow range. They found no enhancement of heat transfer as compared to a flat plate, whereas, in the turbulent zone, the separated shear layer between the recirculation vortex has been developed. In an another study by Nishimura et al. [10] on the wavy channel geometry with much narrower channel spacing. They found no recirculation zone appeared in channel and no flow separation. Okyakawa et al. [11] investigated a wavy channel geometry to determine an optimal channel spacing. They found that the channel spacing as the most important parameter to enhance heat transfer. Asako et al. [12] worked numerically on the triangular corrugated channel and corrugated duct with round corners with the finite volume approach. They found lower friction factors and Nusselt numbers for the corrugated duct with round corners. The amount of enhancement was greatly dependent on the flow conditions and the geometry of the channel. Priyam and Chand [13, 14] studied the effect of mass flow rate and fin spacing, wavelength and amplitude on thermal and thermohydraulic performances of wavy finned absorber solar air heater. Their mathematical model predicted an enhancement of 62.53–63.41% in thermal efficiency and 29.39–29.43% in the effective temperature rise for the

Table 1 System and operating parameters used

Parameters	Value	Parameters	Value
Length of Collector (L)	1200 mm	Mass flow rate ($\dot{m}$)	0.00312–0.0158 kg/s
Width of Collector (W)	400 mm	Fin spacing (w)	2,3,4,5,6 cm
Duct height (H)	50 mm	Thermal conductivity of glass wool (k_{gw})	0.04 W/m-K
Thickness of fin (δ_f)	1 mm	Thickness of insulation (δ_{ins})	50 mm
Actual length of fin (L_{act})	1390 mm	Amplitude of wavy fin (amp)	7.5 mm
Number of glass covers (N_{gc})	1	Wavelength of wavy fin (λ)	70 mm
Height of fin (L_f)	45 mm		

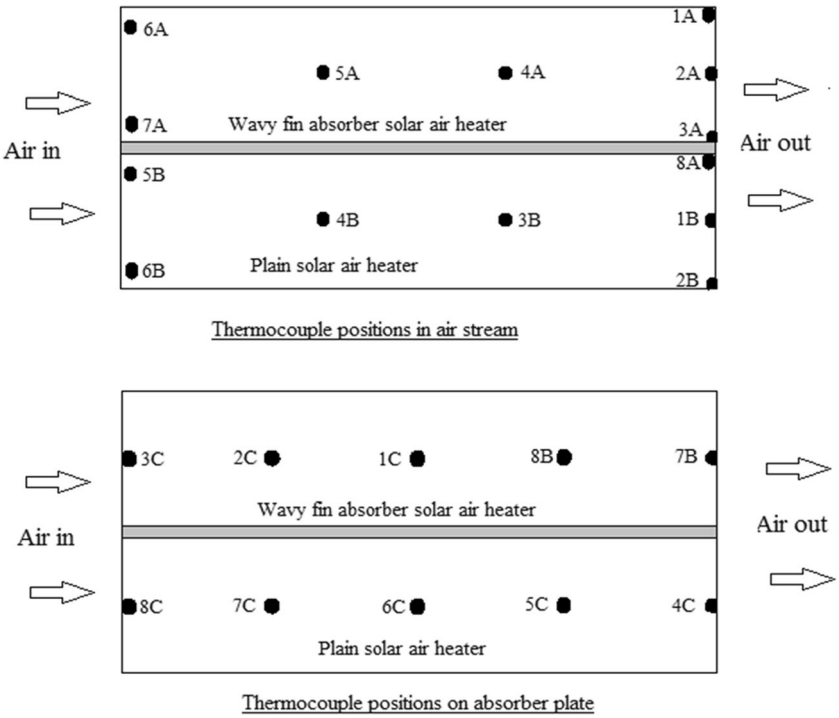

Fig. 2 Positions of thermocouples in air stream and on absorber plate

investigated mass flow range of 0.0138–0.0834 kg/s. In an another study, the effect of the collector aspect ratio has been investigated on the thermal performances of wavy fin absorber solar air heater by Priyam and Chand [15]. They found that the performance of wavy fin solar air heater improved with the increase in the collector aspect ratio.

It is evident from the literature that by providing wavy fins along the fluid flow increases the amount of heat transfer rate by

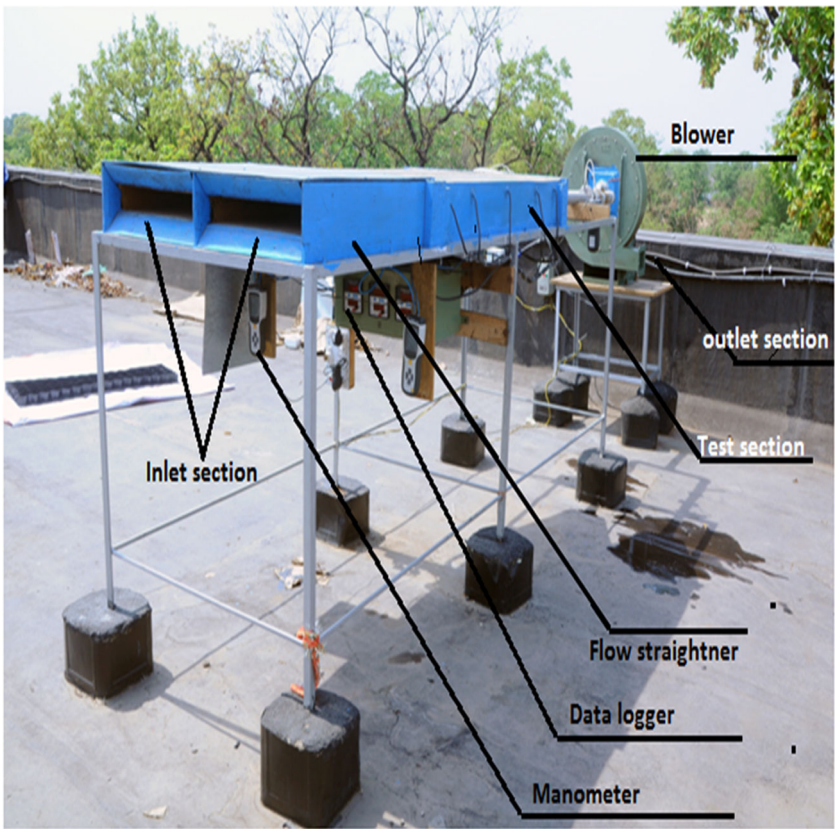

Fig. 3 Photographic view of experimental set up

Fig. 4 Pyramometer with digital output

inceasing the heat transfer area. In the previous works experimental and theoretical investigations were done for the heat exchangers with wavy fins whereas in the wavy fin solar air heater, only theoretical investigations have been done. In the present work, experimental investigation has been carried out on the thermal performance of solar air heater with sinusoidal wavy fins below the absorber. The effect of mass flow rates and the fin spacings on the thermal and thermohydraulic performances and air temperature rise has been studied to design and fabricate for its effective use. Also, the variation of thermal efficiency as a function of temperature rise parameter ($\Delta T/I$) for various fin spacing were examined. The obtained results were compared with results available in the literature.

2 Materials and methodology

2.1 Experimental set up

The experimental set-up consists of a blower, wooden rectangular channel, G.I pipe, orifice meter, flow control valve, digital manometer, J-type thermocouples as shown in Fig. 1. The various system and operating parameters used in the analysis are listed in Table 1. The inner dimensions of the both rectangular channels were 1700 mm × 400 mm × 50 mm. The test section has a length of 1200 mm and the flow straightener of 500 mm as per ASHRAE standards [16]. The side and the middle wall of the channel were of soft wood having thickness 25 mm and 40 mm. The bottom of the channels has a 22 gauge G.I sheet over a 50 mm of glass wool insulation supported by 10 mm plywood at the bottom. G.I sheet acts as an absorber in plane solar air heater, whereas, the wavy fins were attached below the absorber in the wavy finned absorber solar air heater. A total of five absorbers A1, A2, A3, A4 and A5 have been made with the fin spacing 2, 3, 4, 5 and 6 cm respectively. The spacing between the glass cover and the absorber plate is 50 mm. The fins as well as plate were blackened with blackboard paint. The area exposed is 0.48 m^2 for both the collectors. A total of 24 thermocouples was used, out of which 5 were used to measure the plate temperature of each collector and 7 each to measure air temperature inside the duct. The positions of thermocouples over the test section to measure air and plate temperature has been shown in Fig. 2. All thermocouples were connected to a data logger for digital display.

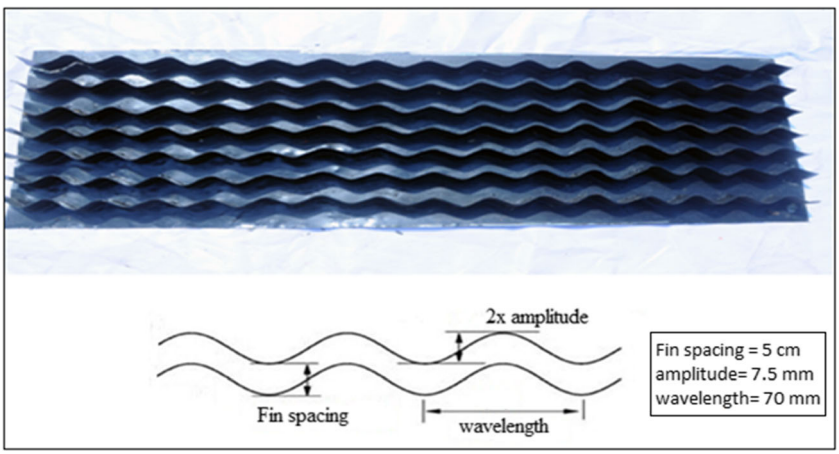

Fig. 5 A typical absorber plate and its specification

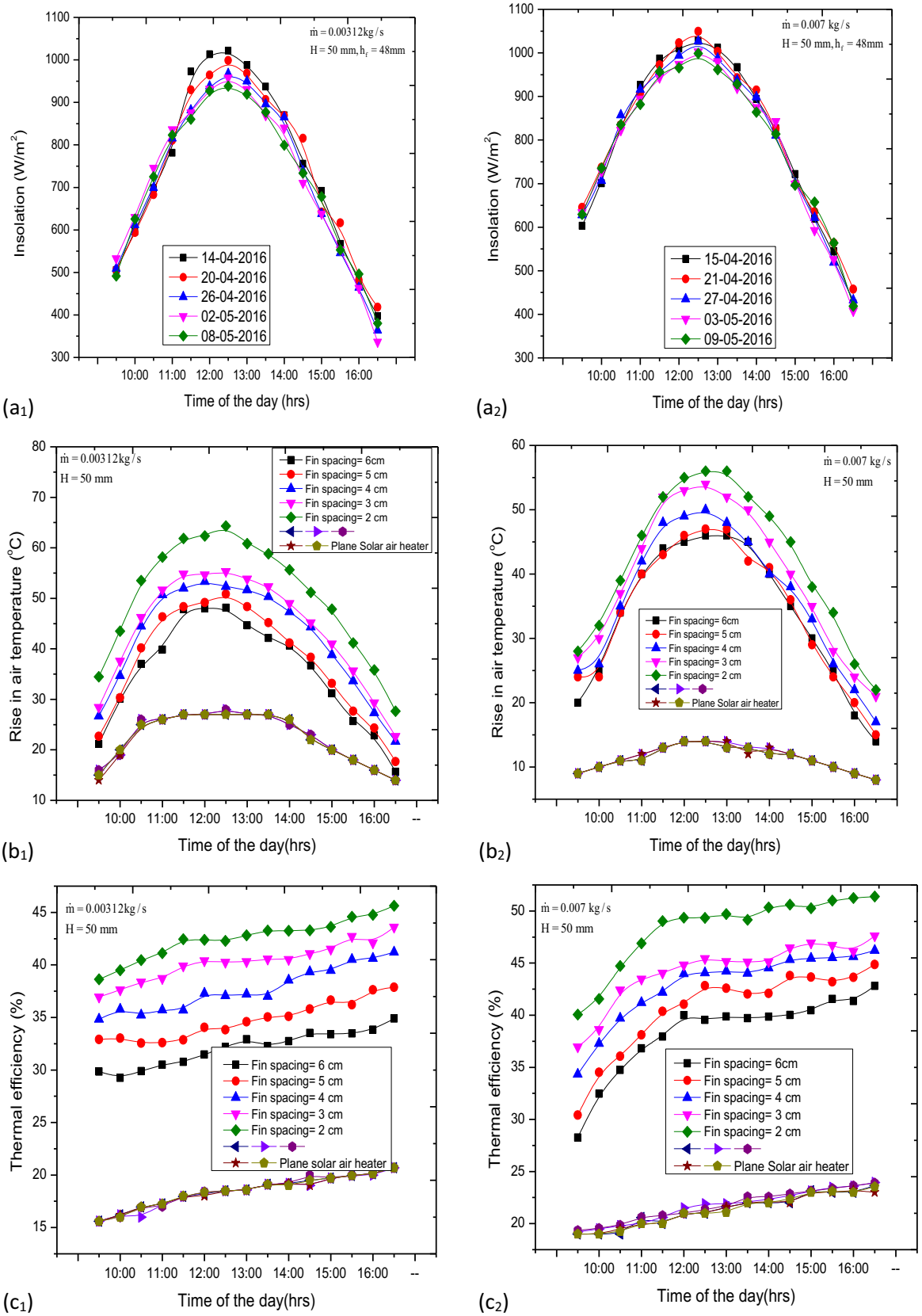

Fig. 6 Variation of (a_1-a_6) insolation, (b_1-b_6) rise in air temperature and (c_1-c_6) thermal efficiency with time at different air flow rates for different fin spacing

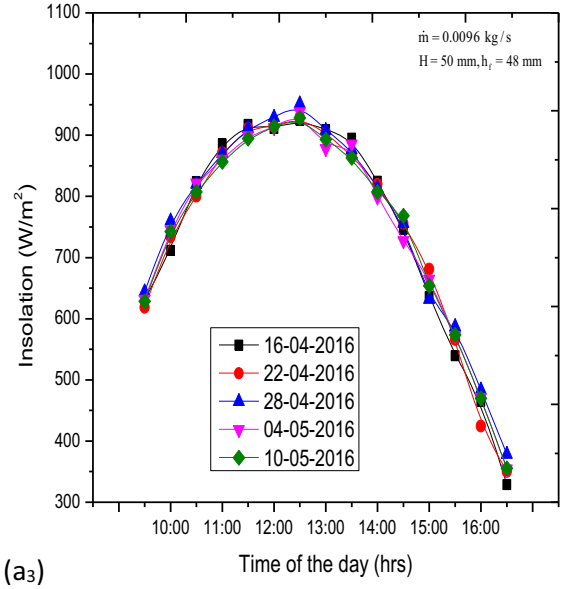

(a3)

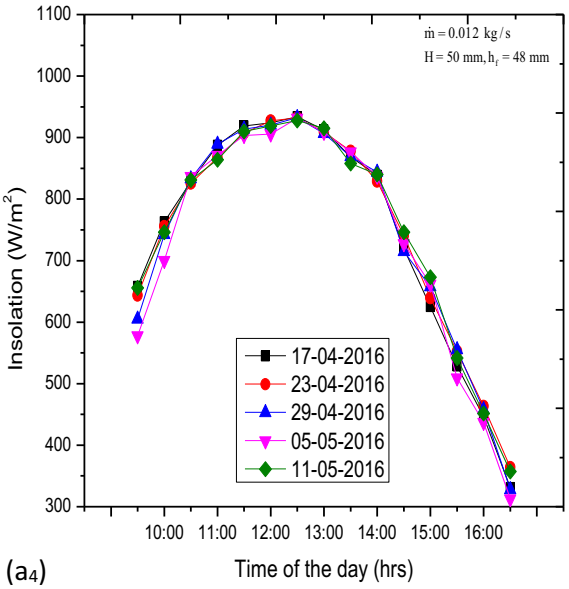

(a4)

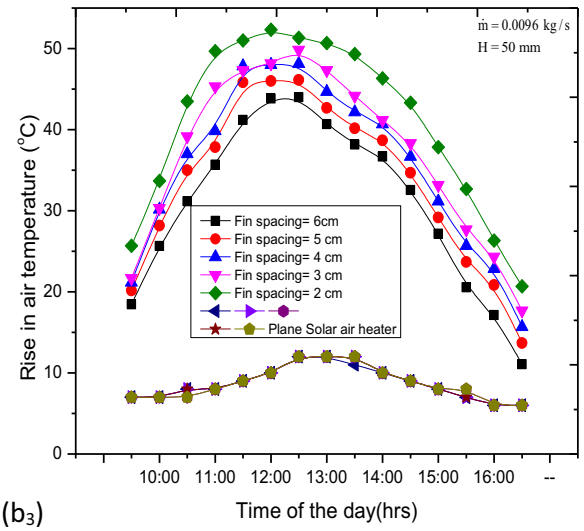

(b3)

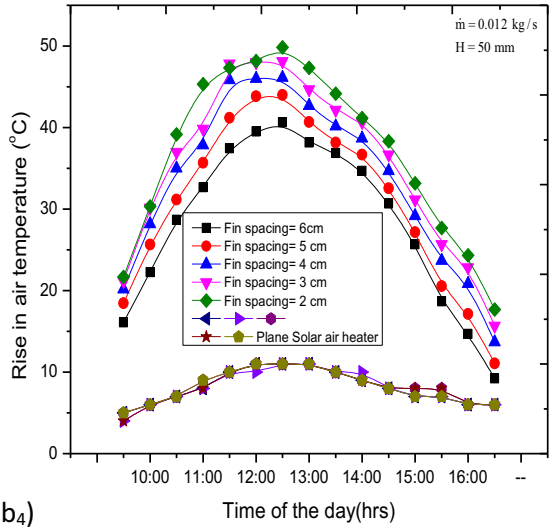

(b4)

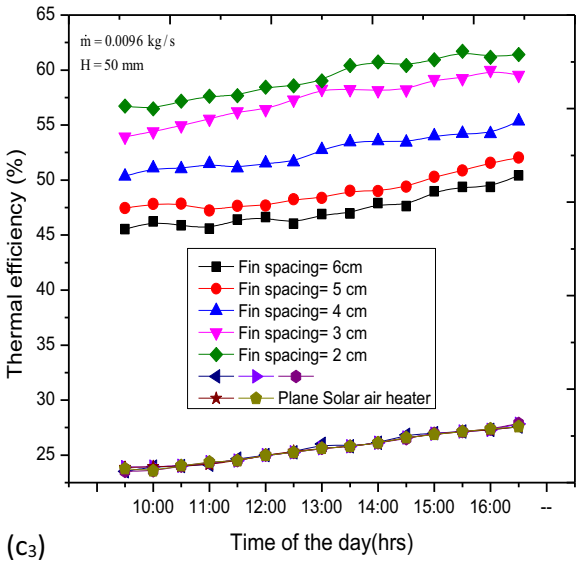

(c3)

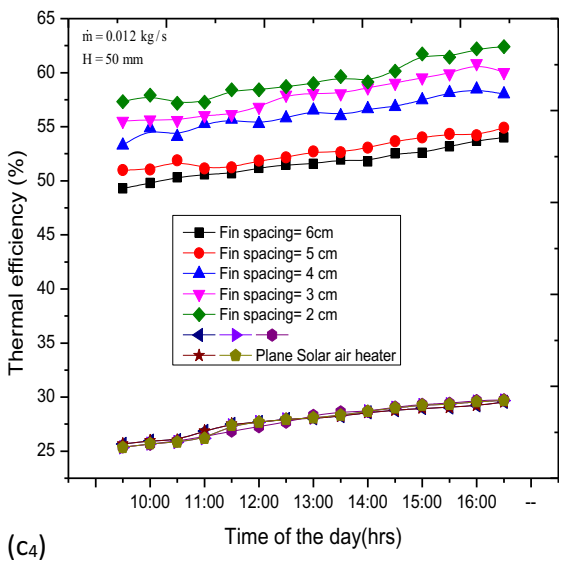

(c4)

Fig. 6 (continued)

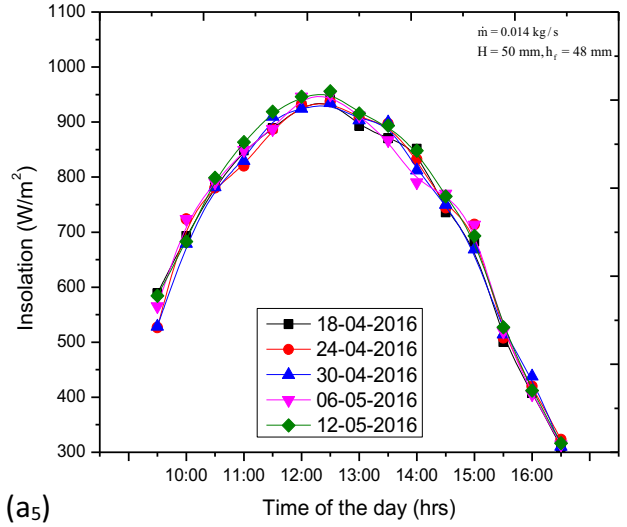

(a5)

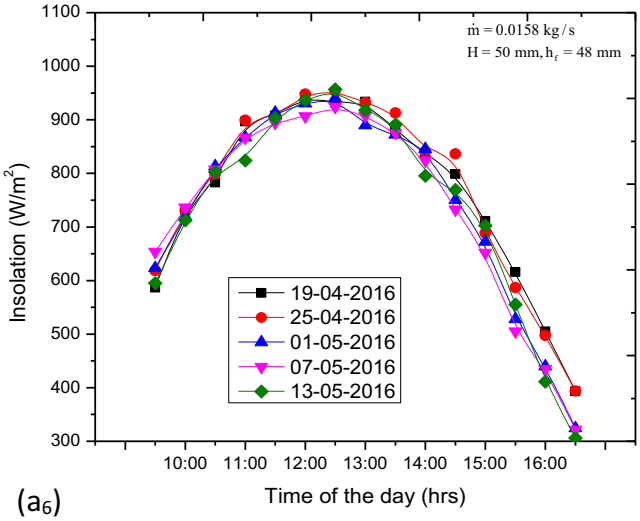

(a6)

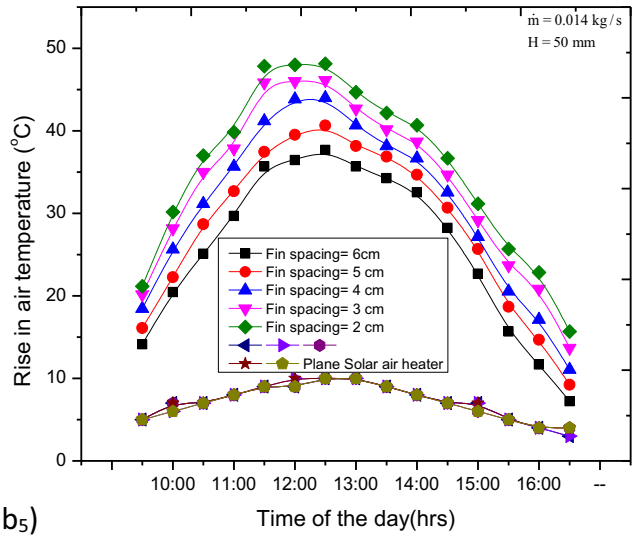

(b5)

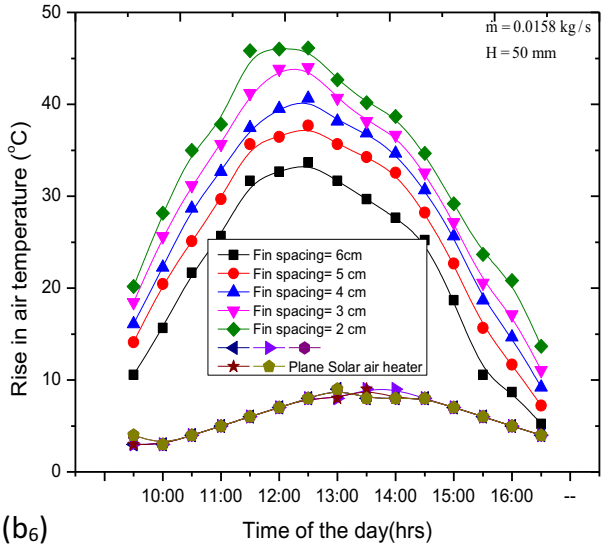

(b6)

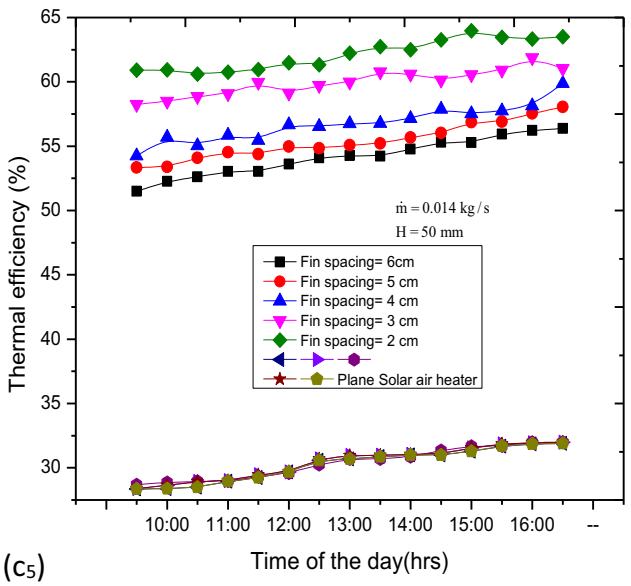

(c5)

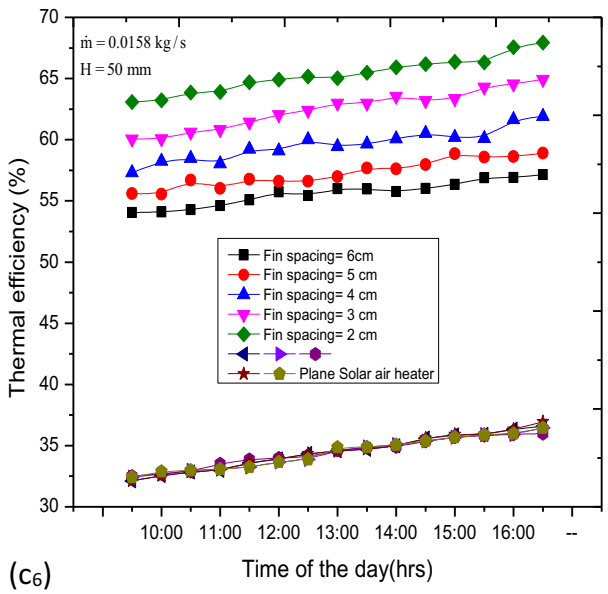

(c6)

Fig. 6 (continued)

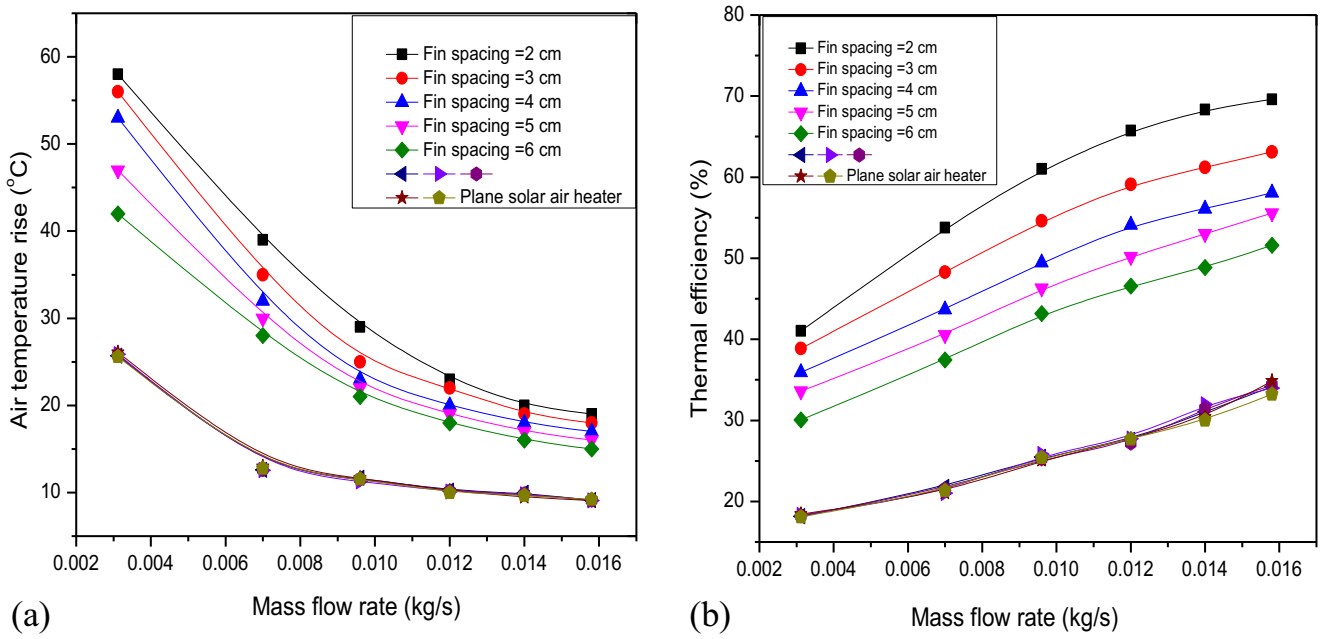

Fig. 7 **a** Air temperature rise and **b** thermal efficiency as a function of mass flow rate for different fin spacing at 12 noon

A total of three data loggers (A,B,C) having 8-channels each has been used to record the temperature. The air mass flow rate flowing through duct was measured by using a calibrated orifice meter fitted with digital manometer. The calibration of orifice meter was done by fitting the orifice meter in series with the calibrated orifice plate with known coefficient of discharge. The outlet of the air heaters were connected to wooden convergent section coupled with G.I pipes, orifice meter, flow control valve and a 3 hp., 3-ph blower. The pictorial view of the experimental set-up is shown in Fig. 3. Insolation was recorded by a pyranometer as shown in Fig. 4 with digital output.

2.2 Experimentation

The wavy fins of known physical characteristics were welded on the absorber plate as shown in Fig. 5 and fitted between the absorber plate and the bottom plate of solar air heater. The collectors were tested in the horizontal position as per ASHRAE-93 standards [16]. Outdoor testing of both plane and wavy fin solar air heater were done on clear sky days. Before the initiation of experimentation, all the components of the set up and the measuring instruments such as data logger, manometer and the pyranometer had been checked for their proper operation. After that the blower was switched on ensuring no leakage in the joints of duct. The mass flow rate in the duct was adjusted using a flow control valve. The blower was adjusted to run 1 h prior to the time at which the first data logging start. The temperature of the various thermocouples, wind speed, manometer reading and insolation were recorded daily at an interval of 30 min from 9:30 am to 4:30 pm. The test was run for a fixed mass flow rate for a specific day. It was decided to take six values of mass flow rates (the partial opening to the full opening of the flow control valve) in order to cover the usual range of mass flow rate and five sets of fin spacing.

2.3 Thermal performance

The thermal performance of flat plate solar air heater operating under quasi steady state conditions can be given by using the following eq. [2];

$$\eta = \frac{\dot{m}C_p(T_o - T_i)}{IA_C} \tag{1}$$

Also, for the solar air heaters taking air at ambient temperature, the following equations for thermal efficiency can be given as [7].

$$\eta = F_0\left[(\tau\alpha)_e - U_L\left(\frac{T_0 - T_i}{I}\right)\right] \tag{2}$$

where, F_0 is the heat removal factor corresponding to outlet air temperature.

Equation shows the plot of efficiency as a function of $(T_0 - T_i)/I$ will result a straight line with slope $-F_0U_L$ and the intercept $F_0(\tau\alpha)_e$. The solar air heaters test data presented as plots of thermal efficiency vs ΔT/I, the intercept $F_o(\tau\alpha)$and slope $-F_oU_L$ of these curves can be converted to F_RU_L, $F_R(\tau\alpha)_e$ and $F'U_L$ by the following and suggested by Duffie & Beckman [2].

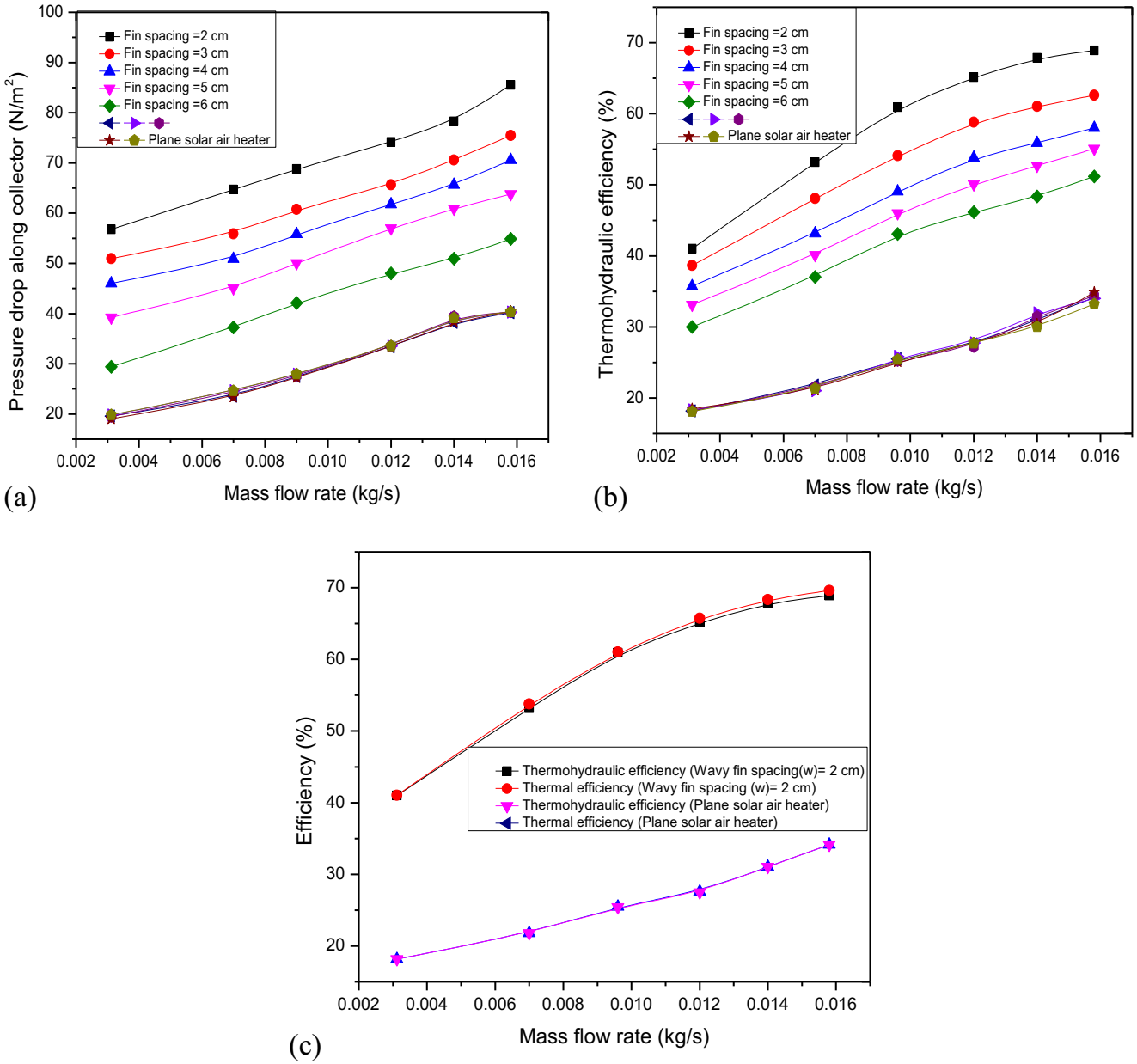

Fig. 8 **a** Pressure drop along collector **b** thermohydraulic efficiency and **c** efficiency as a function of mass flow rate for different fin spacing at 12 noon

$$F_R(\tau\alpha)_e = F_0(\tau\alpha)_e\left(1+\frac{A_c F_0 U_L}{\dot{m}C_P}\right)^{-1} \quad (3)$$

$$F_R U_L = F_0 U_L\left(1+\frac{A_c F_0 U_L}{\dot{m}C_P}\right)^{-1} \quad (4)$$

$$F' U_L = -\frac{\dot{m}C_P}{A_c}\ln\left(1-\frac{F_R U_L A_c}{\dot{m}C_P}\right) \quad (5)$$

The eqs. (1) and (2) can be represented on a single plot having the same quantity, efficiency on ordinate and $(T_0 - T_i)/I$ on abscissa. Also, this can be obtained from a single regression linear fit line from eq. (2).

Also, the error analysis has been done as per the methodology suggested by Kline and Mc Clintock [17] .

2.4 Thermohydraulic performance

The net energy gain, Q_{net}, of the collector can be expressed as the difference between the useful thermal energy gain, Q_u, and the equivalent thermal energy required for producing the work energy necessary to overcome the pressure energy losses. This net energy can be written as,

$$Q_{net} = Q_u - {}^{P_m}/_{C} \quad (6)$$

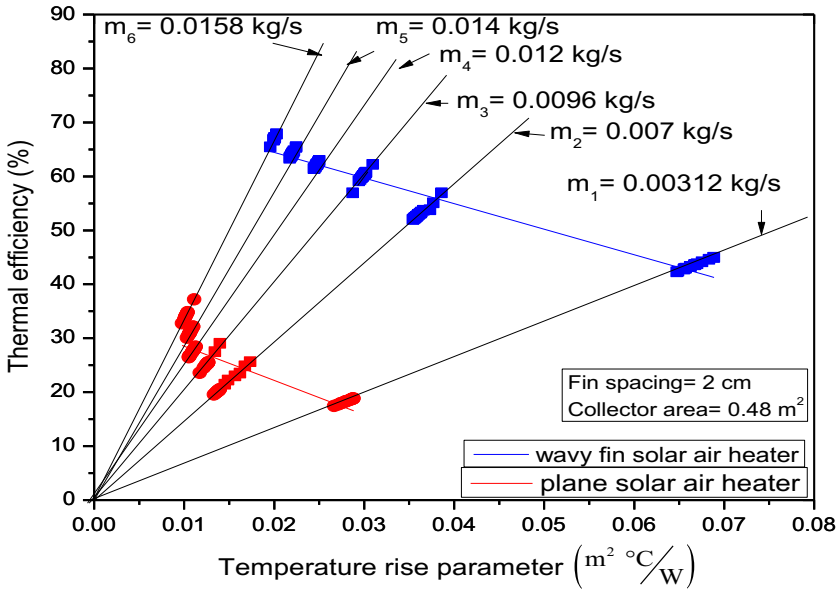

Fig. 9 Performance plot for solar air heater for fin spacing of 2 cm

where, 'P_m' is the mechanical energy consumption to overcome the friction and computed by the relation,

$$P_m = \frac{\dot{m}\Delta P_d}{\rho} \tag{7}$$

where ΔP_d is the pressure drop along the duct and ρ is the density of air entering to the duct. 'C' is the conversion factor representing conversion from thermal energy to compression energy of the fan / blower imparted to air [13] and given as $C = \eta_{Th}\eta_{tr}\eta_m\eta_f$ and the value of C is taken as 0.189 considering the thermal efficiency of power plant (η_{Th}) as 0.35, transmission efficiency (η_{tr}) as 0.9, motor efficiency (η_m) as 0.8 and fan efficiency (η_f) as 0.75.

Thermohydraulic performance is the performance of a system that includes the consideration of thermal as well as hydraulic characteristics. It is necessary to take electrical energy required for pumping into account, while evaluating the performance of solar air heater. From second law of thermodynamics considerations, the power from the thermal output of the collector, always looses a considerable part of the energy in conversion and transmission. Therefore, the pumping power required is converted to equipment thermal energy to obtain the evaluated real performance of the collector in terms of the

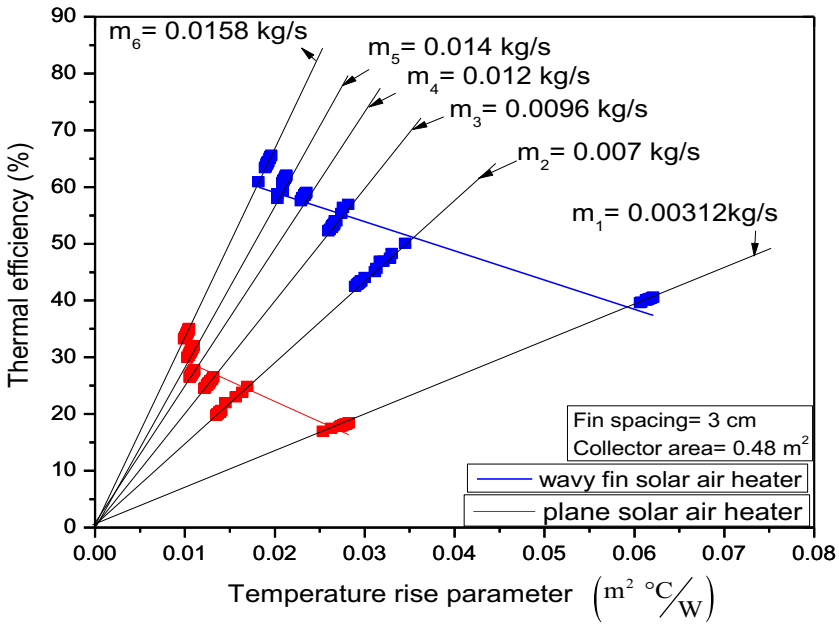

Fig. 10 Performance plot for solar air heater for fin spacing of 3 cm

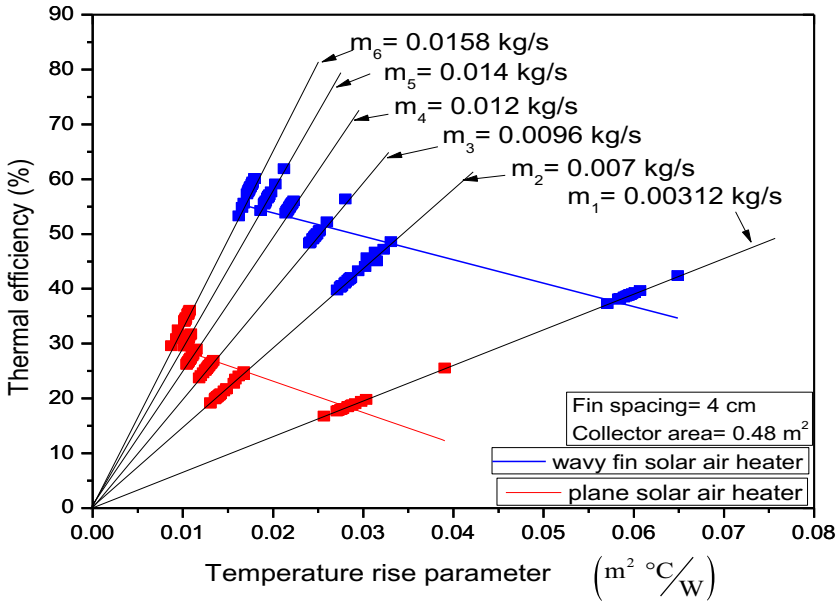

Fig. 11 Performance plot for solar air heater for fin spacing of 4 cm

effective efficiency that takes into account the useful thermal gain and equivalent thermal energy required to provide corresponding mechanical energy for overcoming friction power losses, and is given by,

$$\eta_{eff} = \frac{Q_{net}}{I \text{ x } A_C} \tag{8}$$

Also, the thermohydraulic performance parameter (effective efficiency) can now be written using eqs. (6–8) as,

$$\eta_{eff} = \frac{Q_u - {}^{P_m}/_{C}}{I \text{ x } A_c} \tag{9}$$

2.5 Error analysis

Although extreme care has been taken to perform experiments but there is always a chance of error in experimental measurements. So, it is necessary to determine the maximum possible error in the experimental measurements. The error analysis was done for the error interval associated with experimental results. The methodology suggested by Kline and Mc clintock [17] has been used to measure the error.

If the value of any parameter is calculated using certain measured quantities then error in measurement of 'φ' (parameters) is given as:

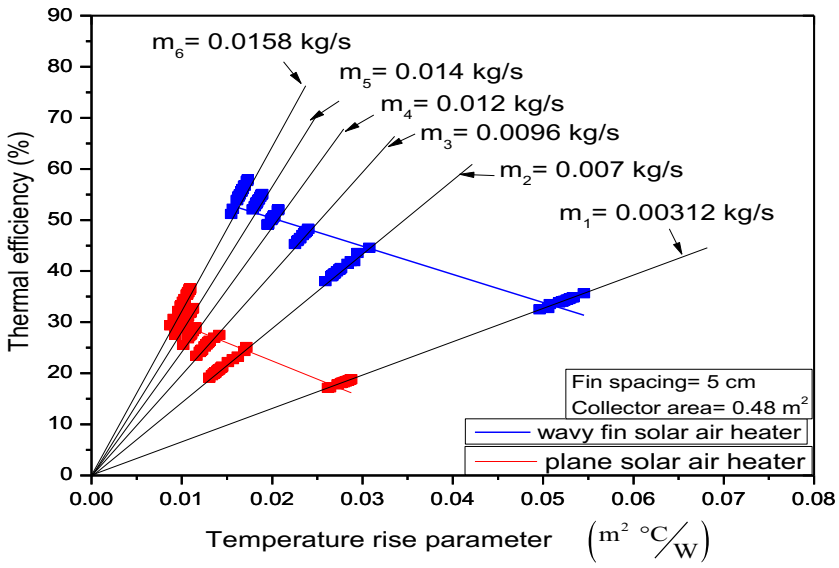

Fig. 12 Performance plot for solar air heater for fin spacing of 5 cm

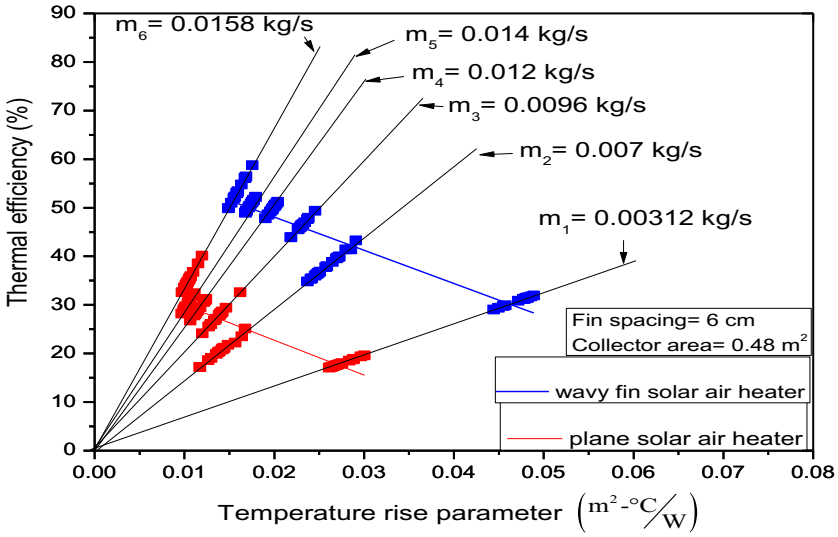

Fig. 13 Performance plot for solar air heater for fin spacing of 6 cm

$$\frac{\delta\varphi}{\varphi} = \left[\left(\frac{\delta\varphi}{\partial x_1}\delta x_1\right)^2 + \left(\frac{\delta\varphi}{\partial x_2}\delta x_2\right)^2 + \ldots\ldots\ldots\ldots + \left(\frac{\delta\varphi}{\partial x_n}\delta x^n\right)^2\right]^{0.5} \quad (10)$$

where, δx_1, δx_2, δx_3.....δx_n are the possible errors in measurements x_1, x_2, x_3....x_n and$\delta\varphi$ is called as absolute uncertainty and $\delta\varphi/\varphi$ is known as relative uncertainty. The fractional error analysis of the mass flow rate and the efficiency are found to be 0.0743 and 0.013 respectively.. Also, Table 6 shows the accuracy of measuring instruments.

3 Results and discussion

This experimental work investigates the effect of fin spacing of wavy finned absorber solar air heater under Jamshedpur, India weather between 14 and 04-2016 to 13-05-2016 with clear sky conditions. Jamshedpur city of India lies on the geographical coordinates of 22° 48' N, 86° 11′ E. Table 1 shows the system and operating parameters used for the analysis.

Figure 6 shows the variation of insolation versus local time of all the days at which the study was conducted. As expected, the insolation increased from sunrise to peak at noon and then decreased in the afternoon till sunset. The average values of insolation for the experiments of 2, 3, 4, 5 and 6 cm spacing were 861.89, 872.29, 869.02, 867.2 and 858.3 W/m^2 respectively. The measured insolation were stable throughout the study.

Figure 7a shows the air temperature rise at different mass velocities for 2, 3, 4, 5 and 6 cm fin spacing. As expected, for each cases, the value of the air temperature rise increases at sun rise to a maximum value at noon and start decreasing in the afternoon. Also, rise in temperature decreases with

Table 2 Experimental values of thermal efficiencies from regression best fit lines

Type of Absorber	Fin Spacing (cm)	Mass flow rate (kg/s)	Efficiency of plane solar air heater (%)	Efficiency of wavy fin solar air heater (%)	Enhancement in efficiency (%)
A1	2	0.00312	18.2	40.1	120.33
		0.0158	29.4	65.1	121.43
A2	3	0.00312	18.6	38.4	106.45
		0.0158	30	59.7	99
A3	4	0.00312	18.4	35.6	93.48
		0.0158	29.6	55.4	87.16
A4	5	0.00312	17.6	31.6	79.54
		0.0158	30	52.3	74.33
A5	6	0.00312	16.3	28.6	75.46
		0.0158	30.1	50.4	67.44

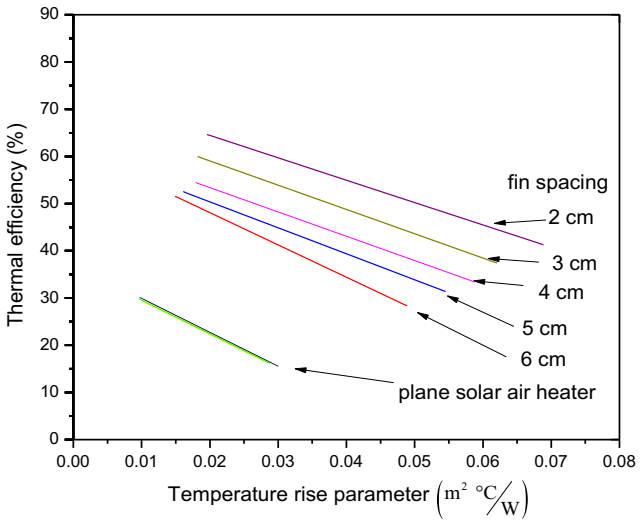

Fig. 14 Performance plot for solar air heaters

Table 3 Heat transfer coefficient and overall heat conductance

Type of Absorber	Fin Spacing (cm)	Mass flow rate (kg/s)	Heat transfer coefficient of plane solar air heater (W/m^2-K)	Heat transfer coefficient of wavy fin solar air heater (W/m^2-K)	Overall Heat conductance of wavy fin solar air heater (W/K)
A1	2	0.00312	3.221	9.112	27.062
		0.0158	7.914	29.801	88.508
A2	3	0.00312	3.222	6.192	12.483
		0.0158	7.894	20.345	41.015
A3	4	0.00312	3.211	4.852	8.049
		0.0158	7.914	15.782	26.182
A4	5	0.00312	3.231	4.082	5.714
		0.0158	7.849	13.301	18.621
A5	6	0.00312	3.221	3.591	4.309
		0.0158	7.927	11.741	14.089

increasing mass flow rate. The maximum value of the air temperature rise was achieved between 12:00 h to 13:00 h of local time and varied in magnitude for each day depending on the meteorological conditions such as wind speed and insolation. It also finds that the rise in air temperature increased by decreasing the fin spacing for the same mass flow rate. As the fin spacing decreased, the velocity of air also increased for the same mass flow rate. The highest average and instantaneous peak rise in air temperature obtained for lowest fin spacing (2 cm) were 50.47°C and 64.33°C respectively, with a mass flow rate of 0.00312 kg/s, whereas, the average and the maximum value of the air temperature rise obtained for maximum mass flow rate of 0.0158 kg/s were 33.51°C and 46.13°C, respectively. On the other hand, higher value of fin spacing (6 cm), the average and instantaneous peak rise in air temperature were obtained as 35.44°C and 48.13°C for lower mass flow rate (0.00312 kg/s) and 25.80°C and 37.68°C for higher mass flow rate (0.0158 kg/s) respectively.

At the lower mass flow rates the convective heat transfer coefficient is small owing to low value of superficial velocity of air and the top surface result in higher amount of thermal losses and hence lower thermal efficiency of the collector. The

Table 4 Collector performance parameters

Fin Spacing (cm)	$F_0(\tau\alpha)_e$	$-F_0U_L$	F_0
2	0.7391	4.74	0.865
3	0.6933	5.14	0.812
4	0.6479	5.48	0.759
5	0.6140	5.51	0.719
6	0.5971	6.82	0.692

pressure drop along the collector has been experimentally evaluated for all the systems and has been shown in Fig. 8a for various fin spacings and duct heights. As the mass flow rate increases the friction factor increases and thus increase in pressure drop. Figure 8b show that thermohydraulic efficiency increases upto maxima and thereafter starts decreasing for all values of fin spacings. Thermohydraulic efficiency represents the net useful thermal energy gain, taking account of the thermal energy required to produce the work - energy necessary to overcome additional friction or hydraulic loss. Figure 8c show the variations in thermal and thermohydraulic efficiencies as a function of the mass flow rate of air. The thermohydraulic and thermal efficiencies increase with an increase in the mass flow rate of air but thermohydraulic efficiency of wavy fin attains a maximum and subsequently decreases with further increase in mass flow rate. This may be attributed to the lower amount of energy spent in overcoming the friction losses at the lower mass flow rates. The energy required to overcome friction losses increases sharply with increase in mass flow rates; the rate of increase of heat transfer and friction losses are in fact, not proportional, i.e., the heat transfer coefficient increase being proportional to a power less than one of the mass flow rate, while the friction losses increasingly with the square of the mass flow rate. Consequently, at higher mass flow rate, the rate of increase of heat transfer is lower in comparison to the rate of increase of friction losses, i.e., a region where the actual gains are not commensurate with expenditure in power loss.

Figures 9, 10, 11, 12 and 13 show the experimental values of thermal efficiencies as a function of air temperature rise parameter, i.e.; $(T_o\text{-}T_i)/I$ or $\Delta T/I$ of plane and wavy finned absorber solar air heater for various fin spacings. Each line of these figures has been obtained from the linear regression fit of the data for the corresponding fin spacings of the wavy fin absorber solar air heater. Also, the plot for the plane solar air heater has been done for the comparison. The plot shows the increased thermal efficiency with the increase in mass flow rate for the both plane as well as wavy fin absorber solar air heaters. It is seen from Fig. 9 that the efficiency of plane solar air heater increases from 18.54% to 29.2% as the mass flow rate increases from 0.00312 kg/s to 0.0158 kg/s. The corresponding values of thermal efficiency for wavy finned absorber has been obtained as 40% to 65%. These values of efficiencies refer to the regression linear fit lines, whereas, the actual values have been found to vary for each mass flow rate with the variation of $(T_o\text{-}T_i)/I$ or $\Delta T/I$ for a specific mass flow rate. For the mass flow rate of 0.00312–0.0158 kg/s and fin spacing of 2 cm, regression linear fit line show an enhancement in thermal efficiency of 2.15–2.23 times in thermal efficiency as compared to plane solar air heater. For the various fin spacing of wavy fin solar air heater and plane solar air heater, the value of thermal efficiencies and the respective enhancement in thermal efficiency obtained from the respective regression linear fit lines have been listed in Table 2. It shows that the fin

Table 5 Collector performances as a function of mass flow rates

Fin Spacing (cm)	Mass flow rate (kg/s)								
	0.00312			0.012			0.0158		
	$F_R(\tau\alpha)_e$	F_RU_L	$F^{'}U_L$	$F_R(\tau\alpha)_e$	F_RU_L	$F^{'}U_L$	$F_R(\tau\alpha)_e$	F_RU_L	$F^{'}U_L$
2	0.7339	4.707	5.69	0.7374	4.730	5.36	0.7381	4.734	5.11
3	0.6880	5.105	6.30	0.6916	5.132	5.89	0.6922	5.137	5.58
4	0.6425	5.439	6.82	0.6461	5.470	6.35	0.6468	5.475	5.98
5	0.6089	5.465	6.86	0.6124	5.496	6.38	0.6130	5.502	6.02
6	0.6108	6.281	8.24	0.6151	6.322	8.24	0.6158	6.329	7.03
Plane	0.3452	6.755	8.64	0.3475	6.802	7.54	0.3479	6.810	7.63

spacing of 2 cm have the maximum enhancement in efficiency followed by fin spacing of 3, 4, 5 and 6 cm respectively for all mass velocities.

Figure 14 shows the effect of fin spacing on the thermal performance of wavy fin absorber solar air heater as well as plane solar air heater. The performance lines plotted in the Fig. 13 are the linear regression fit lines of experimental data points of corresponding spacing and represented in Figs. 9-13. Results show that the performance of wavy finned absorber is a strong function of fin spacing .The difference in the performance of these wavy finned solar air heaters is due to the enhanced heat transfer area and the effective heat transfer coefficient between the wavy fin absorber and air. It is clear from Fig. 14 that the fin spacing 2 cm shows the overall best performance followed by fin spacing 3 cm, 4 cm, 5 cm and 6 cm.This is due to the higher value of surface conductance ($\overline{h}$ A) of the lower fin spacing absorb higher energy effectively and transfer more energy to the flowing air. The lower fin spacing, having high value of surface conductance, transfer energy from finned absorber to air more effectively and reduces the absorber plate temperatures and thus reduces the thermal losses from the absorber to the environment, results in enhanced thermal efficiency. The value of heat transfer coefficient $\overline{h}$ and ($\overline{h}$ A) overall heat conductance for the various fin spacing and mass velocities have been listed in Table 3. It can be seen from the table that the overall heat conductance and heat transfer coefficient increases with the decrease in fin spacing for both the minimum and maximum mass velocities. Thus the fin spacing of 2 cm is the most efficient absorber for all mass velocities.

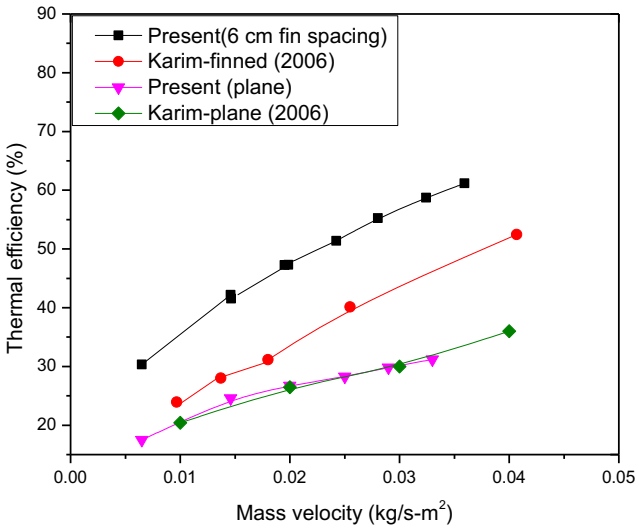

Fig. 15 Thermal efficiency comparison of 6 cm fin spacing solar air heater with some solar air heaters available in literature

The enhancement in thermal efficiency of wavy finned absorber solar air heater as compared to plane solar air heater is found to decrease as the value of ΔT/I increases. The highest value of ΔT/I has been obtained for the lower fin spacing. This enhancement in thermal efficiency of these absorbers appears due to proceeding towards equality of average absorber plate temperature and air and also the decreasing values of absorber plate due to an appreciable rise in the value of overall conductance for the lower fin spacing (2 cm) absorber plate as compare to higher fin spacing (3 cm, 4 cm, 5 cm, and 6 cm).These conditions favours the increase in collector efficiency factor ($F^{'}$) and hence enhanced collector heat removal factor related to outlet fluid temperature (F_o). Also, the value of the overall loss coefficient, U_L will decrease according to Shewan and Hollands [18] who have shown that the overall loss coefficient

Table 6 Accuracy of measuring instruments

Sl. No.	Name of Instrument	Accuracy
1	Pyranometer	±0.5°%
2	Digital Manometer	±0.3%
3	Thermocouple	±1 °C

strongly depends on the mean absorber plate temperature as the collector efficiency factor approaches to unity.

The value of performance parameters $F_o(\tau\alpha)_e$ and F_oU_L obtained from the intercept and slope of regression linear fit lines of various fin spacing are listed in Table 4. Also, the respective value of $F_o$and $U_L$has been calculated by calculating the constant value of $(\tau\alpha)_e$. The value of $(\tau\alpha)_e$ has been calculated as 0.854, which is 1% greater than $(\tau\alpha)$ to include glass cover plate absorptance as suggested by Whiller [19]. The solar air heaters test data presented as plots of thermal efficiency and $(T_0 - T_i)/I$, the intercept and slope can be converted to F_RU_L, $F_R(\tau\alpha)_e$and $F^{'}U_L$by the eqs. (3–5).

The value of these parameters for the various fin spacing as a function of mass flow rate are listed in Table 5. The values of F_R, U_L and $F^{'}$ can be calculated by using a constant value of $(\tau\alpha)_e$=0.854 for the various mass velocities.

Figure 15 shows the thermal efficiency comparison of 6 cm fin spacing with some solar air heater efficiencies available in the literature. The thermal efficiency of wavy fin solar air heater is greater than finned solar air heater used by Karim and Hawlader [20] by 29.63% for the investigated range of system and operating parameters. This may because of the shape of wavy fin, the sinosuidal shape of the fin enhances the heat transfer area as well as heat transfer coefficient more than the plane fin and the plane solar air heater. Also, the thermal efficiency values of Karim and Hawlader [20] for plane solar air heater show a deviation ±3.48% from the plane solar air heater of present result. This holds a good agreement between the experimental values and makes the perfection of data collected through experimentation.

4 Conclusions

An experimental study was conducted to evaluate the thermal performance of wavy fin absorber solar air heater. On the basis of this investigation, it is concluded that the wavy fin solar air heater with the lowest fin spacing (2 cm) performs better than higher fin spacing (6 cm) due to the enhanced heat transfer area by narrowing the channel. Also, the lowest mass flow rate (0.00312 kg/s) leads to higher temperature difference. The effect of insolation has been examined for the various fin spacings and the improved thermal performance of wavy fin solar air heater has been found due to the improved surface conductance of finned absorber plate. An enhancement of 121.43% in thermal efficiency has been achieved in comparison to plane solar air heater and this improvement is a strong function of fin spacing and operating parameter.

Appendix 1: Error analysis

Although extreme care has been taken to perform experiment but there is always a chance of error in experimental measurements. So, it is necessary to determine maximum possible error in the experimental measurements. The error analysis was done for the error interval associated with experimental results. The methodology suggested by cline and Mc clintock [19] has been used to measure the error.

If the value of any parameter is calculated using certain measured quantities then error in measurement of 'φ' (parameters) is given as:

$$\frac{\delta\varphi}{\varphi} = \left[\left(\frac{\delta\varphi}{\partial x_1}\delta x_1\right)^2 + \left(\frac{\delta\varphi}{\partial x_2}\delta x_2\right)^2 + \ldots\ldots\ldots\ldots + \left(\frac{\delta\varphi}{\partial x_n}\delta x^n\right)^2\right]^{0.5}$$

Where δx_1, δx_2, δx_3.....δx_n are the possible errors in measurements x_1, x_2, x_3....x_n and$\delta\varphi$ is called as absolute uncertainty and $\delta\varphi/\varphi$ is known as relative uncertainty. Table 6 shows the accuracy of measuring instruments.

Area of absorber plate

$$A_p = (W \times L)$$

$$\delta Ap = \left[\left(\frac{\delta A_p}{\delta L} \times \delta L\right)^2 + \left(\frac{\delta A_p}{\delta W} \times \delta W\right)^2\right]$$

$$\delta A_p = [W \times \delta l]^2 + [L \times \delta W]^2$$

$$\delta A_p = \left[\left(\frac{W\,x\,\delta L}{W\,x\,L}\right)^2 + \left(\frac{Lx\delta W}{WxL}\right)^2\right]^{0.5} \quad \delta A_p = \left[\left(\frac{1}{1200}\right)^2 + \left(\frac{1}{400}\right)^2\right]^{0.5}$$

$$= 2.63x\ 10^{-3} = 0.263\%$$

Area of Flow

$$A_f = (W \times L_{act}) + n(L_f \times L_{act})$$

$$\delta A_f = \left[\left(\frac{\delta A}{\delta L} \times \delta L\right)^2 + \left(\frac{\delta A}{\delta W} \times \delta W\right)^2 + n\left(\frac{\delta(L_f L_{act})}{\delta L_{act}}\right)^2 + \left(\frac{\delta(L_f L_{act})}{\delta L_{act}} \times L_f\right)^2\right]$$

$$\delta A_f = [W \times \delta l]^2 + [L_{act} \times \delta W]^2 + \eta(L_f \times \delta L_{act})^2 + (L_f L_{act})^2$$

$$\delta A_f = \left(\frac{\delta L_{act}}{L_{act}}\right)^2 + \left(\frac{\delta W}{W}\right)^2 + 7\left[\left(\frac{\delta L_{act}}{L_{act}}\right)^2 + \left(\frac{\delta L_f}{\delta L_f}\right)^2\right]^{0.5}$$

$$\delta A_f = \left[\left(\frac{1}{1390}\right)^2 + \left(\frac{1}{400}\right)^2 + 7\left[\left(\frac{1}{45}\right)^2 + \left(\frac{1}{1390}\right)^2\right]\right]^{0.5}$$

$$\delta A_f = 0.05888$$

$$\delta A_f = 5.888\%$$

Area of orifice meter (A_o)

$$A_0 = \frac{\pi}{4} d_2^2$$

$$\frac{\delta A_o}{\delta d_2} = \frac{2\pi d_2}{4} = \frac{\pi d_2}{2}$$

$$\delta A_o = \left(\frac{\pi d_2}{2}\right) \delta d_2$$

$$\frac{\delta A_o}{A_o} = \frac{\pi d_2 \delta d_2 \times 4}{2 \times \pi \times d_2^2} = \frac{2\delta d_2}{d_2} = \frac{2 \times (0.05)}{19} = 0.526\%$$

Mass flow rate ($\dot{m}$)

$$\dot{m} = C_d A_0 \left[\frac{2\rho \Delta P}{1-\beta^4}\right]^{0.5}$$

$$\frac{\delta \dot{m}}{\dot{m}} = \left[\left(\frac{\delta C_d}{C_d}\right)^2 + \left(\frac{\delta A_0}{A_0}\right)^2 + \frac{1}{4}\left(\frac{\delta \rho}{\rho}\right)^2 + \frac{1}{4}\left(\frac{\delta(\Delta P)}{(\Delta P)}\right)^2 + \frac{1}{4}\left(\frac{\delta \beta}{\beta}\right)^2\right]^{0.5}$$

$$= \left[(0.016)^2 + (0.00526)^2 + \frac{1}{4}(0.0083)^2 + \frac{1}{4}\left(\frac{1}{25}\right)^2 + \frac{1}{4}(0.00121)^2\right]^{0.5}$$

$$= 0.0437 \; or \; 4.37\%$$

Useful heat gain (Q_u)

$$Q_u = \dot{m} C_p (T_o - T_i)$$

$$\frac{\delta Q_u}{Q_u} = \left[\left(\frac{\delta \dot{m}}{\dot{m}}\right)^2 + \left(\frac{\delta Cp}{Cp}\right)^2 + \left(\frac{\delta(\Delta T)}{(\Delta T)}\right)^2\right]^{0.5}$$

$$= \left[(0.0437)^2 + (1/1005)^2 + (0.5/15.2)^2\right]^{0.5}$$

$$= 0.0547 \; or \; 5.47\%$$

Heat transfer coefficient ($\overline{h}$)

$$\overline{h} = \frac{Q_u}{A_p (T_{pm} - T_{fm})}$$

$$\frac{\delta \overline{h}}{\overline{h}} = \left[\left(\frac{\delta Q_u}{Q_u}\right)^2 + \left(\frac{\delta A_p}{A_p}\right)^2 + \left(\frac{\delta T_{pf}}{T_{pf}}\right)^2\right]^{0.5}$$

$$= \left[(0.0547)^2 + (0.00358)^2 + \left(\frac{1}{12}\right)^2\right]^{0.5}$$

$$= 0.09974 \text{ or } 9.974\%$$

References

1. Sukhatme SP, Nayak JK (1996) Principles of Thermal Collection and Storage, 2nd edn. Tata Mc Graw Hill Education, New Delhi
2. Duffie JA, Beckman WA (1980) Solar Engineering of Thermal Processes. Wiley, New York
3. Xiao L, Wu S-Y, Zhang Q-L, Li Y-R (2012) Theoretical investigation on thermal performance of heat pipe flat plate solar collector with cross flow heat exchanger. Heat Mass Transf 48(7):1167–1176
4. Hesselgreaves JE (2001) Compact Heat Exchangers: Selection, Design and Operation. Elsevier Science Pvt. Ltd., Cambridge
5. Junqi D, Chen J, Chen Z, Zhou Y, Wenfeng Z (2007) Heat transfer and pressure drop correlations for the wavy fin and flat tube heat exchangers. Appl Therm Eng 27(11–12):2066–2073
6. Snyder B, Li KT, Wirtz RA (1993) Heat Transfer Enhancement in a Serpentine Channel. Int J Heat Mass Transf 36:2965–2976
7. Kays WM, London AL (1984) Compact Heat Exchangers, 3rd edn. McGrawHill, New York
8. Garg VK, Maji PK (1988) Flow and Heat Transfer in a Sinusoidally Curved Channel. International Journal of Engineering Fluid Mechanics 1:293–319
9. Nishimura T, Kajimoto Y, Tarumoto A, Kawamura Y (1986) Flow Structure and Mass Transfer For a Wavy Channel in Transitional Flow Regime. J Chem Eng Jpn 19:449–455
10. Nishimura T, Yoshino T, Kawamura Y (1987) Instability of Flow in a Sinusoidal Wavy Channel With Narrow Spacing. J Chem Eng Jpn 20:102–104
11. Oyakawa K, Shinzato T, Mabuchi I (1989) The Effects of the Channel Width on Heat-Transfer Augmentation in a Sinusoidal Wave Channel. JSME Int J 32:403–410
12. Asako Y, Nakamura H, Faghri M (1988) Heat Transfer and pressure drop characteristics in a corrugated duct with rounded corners. International Journal of Heat Transfer 31:1237–1245
13. Priyam A, Chand P (2016) Thermal and thermohydraulic performanceof wavy finned absorber solar air heater. Sol Energy 130:250–259
14. Priyam A, Chand P (2018) Effect of wavelength and amplitude on the performance of wavy finned absorber solar air heater. Renew Energy 119:690–702
15. Priyam, A. Chand, P.2016. Effect of collector aspect ratio on the thermal performance of wavy finned absorber solar air heater. Energy and Power Engineering. 10(5). 562–566. waset.org
16. ASHRAE standard 93-77 (ANSI B 1981-1977) (1977) Methods of Testing to Determine the Thermal Performance of Solar Collectors. ASHRAE, New York
17. Kline SJ, McClintock FA (1953) Describing Uncertainties in Single Sample Experiments. Mech Eng 75:3–8
18. Shewen EC, Hollands KGT (1979) Equations for presenting the U_t-dependence in collector test procedures. Proceedings of Int. Solar Energy Society, Atlanta, pp 360–364
19. Whiller A (1967) Design factors influencing solar collector performance. In: Jordan RC (ed) Low Temperature Engineering Applications of Solar Energy. ASHRAE, New York, p 27
20. Karim MA, Hawlader MNA (2006) Performance investigation of flat, v- corrugated and finned air collectors. Energy 31:452–470